From Micelles to Randomly Connected, Bilayered Membranes in Dilute Block Copolymer Blends

Jonathan H. Laurer,[†] Jennifer C. Fung,[‡] John W. Sedat,[§] Steven D. Smith,[⊥] Jon Samseth,[#] Kell Mortensen,[▽] David A. Agard,[§,∥] and Richard J. Spontak*,[†]

Department of Materials Science & Engineering, North Carolina State University, Raleigh, North Carolina 27695, Graduate Group in Biophysics, University of California, San Francisco, California 94143, Department of Biochemistry and Biophysics, University of California, San Francisco, California 94143, Howard Hughes Medical Institute, University of California, San Francisco, California 94143, Corporate Research Division, The Procter & Gamble Company, Cincinnati, Ohio 45239, Department of Physics, Institute for Energy Technology, N-2007 Kjeller, Norway, and Department of Physics, Risø National Laboratory, DK-4000 Roskilde, Denmark

Received September 12, 1996. In Final Form: January 24, 1997[⊗]

As macromolecular surfactants, diblock copolymers order into a variety of morphologies in the presence of a parent homopolymer. Here, we probe the effects of chemical incompatibility and interfacial rigidity on the morphology of copolymer/homopolymer blends at constant blend composition. Five copolymers, each possessing a random-sequence midblock that is varied from 0 to 40 wt % of the copolymer molecular weight, have been synthesized for this purpose. While copolymer micelles are representative of dilute (homopolymer-rich) blends, complex bilayered morphologies, including vesicles and the anomalous isotropic "sponge" phase, are produced upon increasing the midblock fraction. Small-angle neutron scattering provides a quantitative assessment of characteristic microstructural dimensions, while transmission electron microtomography yields the first three-dimensional images of the randomly connected, bilayered membrane comprising the sponge phase.

Polymeric materials capable of forming ordered microstructures can be rationally tailored for specific applications through segmental/molecular design accompanied by an understanding of microstructural development. Diblock copolymers, composed of two long contiguous sequences of chemically dissimilar monomers, constitute excellent examples of such materials and likewise represent the macromolecular analogs of low-molar-mass surfactants.[1−9] While diblock copolymers and surfactants order into similar periodic morphologies under suitable conditions, one phase of interest in surfactant-containing systems, but not previously observed in copolymer blends with other polymers, is the anomalous isotropic *sponge* phase. Exhibiting unique flow and optical properties,[3,10−15] this phase consists of a randomly connected, continuous membrane. Although the sponge, or L_3, phase possesses a relatively narrow stability threshold in binary surfactant (/cosurfactant) solutions, it has recently received considerable attention due to its unusual viscosity and flow birefringence properties.[3,14,16−18] By constituting an experimentally accessible example of a self-avoiding, randomly oriented liquid surface, the L_3 phase also helps to elucidate amphiphile aggregation mechanisms,[14,15,18] condensed-matter phase transitions,[12,19−21] and elementary-particle physics.[22]

The L_3 phase arises when the L_α (or lamellar) phase, comprised of alternating bilayers, is sufficiently dilute so that long-range positional and orientational (smectic) order is lost, but a bilayered membrane remains intact.[20] Spatial symmetry of the L_3 phase depends on the relative volume on each side of the membrane. The *symmetric* phase can be described as a randomly interpenetrating membrane of maximal interface dividing comparable interior and exterior volumes.[10−12,14,21] Disparity between these volumes results in the *asymmetric* L_3 phase, possibly composed of unilamellar vesicles in the dilute regime.[14,15] Existence of the L_3 phase has been established in surfactant systems primarily through the use of indirect experimental methods, including small-angle scattering.[10,11,23] While real-space morphological information of

* To whom correspondence should be addressed.
[†] Department of Materials Science & Engineering, North Carolina State University.
[‡] Graduate Group in Biophysics, University of California.
[§] Department of Biochemistry and Biophysics, University of California.
[⊥] Corporate Research Division, The Procter & Gamble Co.
[#] Department of Physics, Institute for Energy Technology.
[▽] Department of Physics, Risø National Laboratory.
[∥] Howard Hughes Medical Institute, University of California.
[⊗] Abstract published in *Advance ACS Abstracts,* March 15, 1997.

(1) Bates, F. S. *Science* **1991**, *251*, 898.
(2) Strey, R.; Schömacker, R.; Roux, D.; Nallet, F.; Olsson, U. *J. Chem. Soc., Faraday Trans.* **1990**, *86*, 2253.
(3) Hoffmann, H. *Ber. Bunsenges. Phys. Chem.* **1994**, *98*, 1433.
(4) Bates, F. S.; Fredrickson, G. H. *Annu. Rev. Phys. Chem.* **1990**, *41*, 525.
(5) Förster, S.; Khandpur, A. K.; Zhao, J.; Bates, F. S.; Hamley, I. W.; Ryan, A. T.; Bras, W. *Macromolecules* **1994**, *27*, 6922.
(6) Schulz, M. F.; Bates, F. S.; Almdal, K.; Mortensen, K. *Phys. Rev. Lett.* **1994**, *73*, 86.
(7) Hajduk, D. A.; Harper, P. E.; Gruner, S. M.; Honeker, C. C.; Kim, G.; Thomas, E. L.; Fetters, L. J. *Macromolecules* **1994**, *27*, 4063.
(8) Matsen, M. W. *Macromolecules* **1995**, *28*, 5765.
(9) Spontak, R. J.; Fung, J. C.; Braunfeld, M. B.; Sedat, J. W.; Agard, D. A.; Kane, L.; Smith, S. D.; Satkowski, M. M.; Ashraf, A.; Hajduk, D. A.; Gruner, S. M. *Macromolecules* **1996**, *29*, 4494.
(10) Porte, G.; Marignan, J.; Bassereau, P.; May, R. *J. Phys. (Paris)* **1988**, *49*, 511.
(11) Marignan, J.; Appell, J.; Bassereau, P.; Porte, G.; May, R. P. *J. Phys. (Paris)* **1989**, *50*, 3553.
(12) Roux, D.; Coulon, C.; Cates, M. E. *J. Phys. Chem.* **1992**, *96*, 4174.
(13) Hoffmann, H.; Thunig, C.; Munkert, U.; Meyer, H. W.; Richter, W. *Langmuir* **1992**, *8*, 2629.
(14) Cates, M. E. *Philos. Trans. R. Soc. London* **1993**, *A 344*, 339.
(15) Safran, S. A. In *Micelles, Membranes, Microemulsions, and Monolayers*; Gelbar, W. M., Ben-Shaul, A., Roux, D., Eds.; Springer-Verlag: New York, 1994; pp 451−474.
(16) Nilsson, P. G.; Lindman, B. *J. Phys. Chem.* **1984**, *88*, 4764.
(17) Diat, O.; Roux, D. *Langmuir* **1995**, *11*, 1392.
(18) Granek, R.; Cates, M. E. *Phys. Rev. A* **1992**, *46*, 3319.
(19) Cates, M. E. *Physica A* **1991**, *176*, 187.
(20) Coulon, C.; Roux, D.; Bellocq, A. M. *Phys. Rev. Lett.* **1991**, *66*, 1709.
(21) Antelmi, D. A.; Kékicheff, P.; Richetti, P. *J. Phys. II* **1995**, *5*, 103.
(22) David, F. *Europhys. Lett.* **1989**, *9*, 575.
(23) Hecht, E.; Mortensen, K.; Hoffmann, H. *Macromolecules* **1995**, *28*, 5465.

S0743-7463(96)00887-6 CCC: $14.00

the bilayered L_3 phase in binary systems, as well as its more common (but monolayered) analog in surfactant/oil/water ternary microemulsions,[24] is required to ascertain the spatial arrangement of the dividing membrane, such information remains relatively scarce.[3,13]

Visualization of the L_3 microstructure has traditionally relied on freeze-fracture/replication transmission electron microscopy (FF/TEM), since this phase has thus far been limited to aqueous systems containing either low-molar-mass or, more recently, macromolecular[23] surfactants. Cryogenic fracture/replication is, however, prone to specimen-preparation artifacts, and FF/TEM micrographs only provide two-dimensional (2-D) information from fracture surfaces. By systematically varying the monomer sequence pattern (i.e., molecular architecture) in a series of compositionally symmetric, extended block copolymers (depicted in terms of repeat units A and B in Scheme 1), we have successfully generated the L_3 phase in dilute block

Scheme 1

···AAAA(BBABAABBA···BAABBABAA)BBBB···

copolymer blends with a parent homopolymer. Formation of this phase in a thermoplastic-rich polymer blend that is principally a glassy solid at ambient temperature greatly facilitates in-depth morphological analysis through the use of electron microtomography. Electron microtomography, unlike FF/TEM, can provide 3-D volume reconstructions of complex 3-D microstructures with no assumptions of symmetry nor requirements for crystallinity. As shown in this work, this approach affirms that block copolymer and surfactant molecules self-organize into layered microstructures in the dilute regime by comparable, *if not identical*, mechanisms, thereby providing additional evidence that block copolymers and surfactants are governed by universal self-organization principles.

Five linear styrene−isoprene block copolymers, each with a 25% deuterated styrene endblock, and a homopolystyrene (hPS) were synthesized via living anionic polymerization. A poly(styrene-*b*-isoprene) diblock copolymer and a 20 000 (number-average molecular mass) hPS were prepared with *sec*-butyllithium in cyclohexane, whereas a *sec*-butyllithium/potassium alkoxide cocatalyst was used to prepare four extended poly[styrene-*b*-(styrene-*r*-isoprene)-*b*-isoprene] copolymers with random midblocks (each 50/50 (w/w) styrene/isoprene). In this series, the midblock was varied from 10 to 40 wt %, in 10 wt % increments, of the overall copolymer molecular weight. To facilitate discussion, these copolymers are hereafter designated as SI*x*, where *x* denotes the midblock concentration in wt %. According to ^{1}H NMR, the copolymers studied here were all 50 wt % styrene, and from gel permeation chromatography, their number-average molecular masses ranged from 141 000 to 160 000. Binary copolymer/homopolymer blends produced at an overall concentration of 90 wt % styrene were cast from toluene, dried slowly for 3 weeks, and annealed to promote microstructural equilibration.

Upon solution casting from toluene and postannealing, dried films of the blends were first sectioned at −100 °C on a Reichert-Jung Ultracut-S cryoultramicrotome and then selectively stained with the vapor of 2% OsO_4(aq) for 90 min so that the unsaturated isoprene-rich regions would appear electron-opaque (dark). Images were acquired on a Zeiss EM902 electron spectroscopic microscope operated at 80 kV and $\Delta E = 50-100$ eV. Cryosections for electron microtomography were surface-decorated with 15 nm colloidal gold beads, and 53 images of the same region from the same specimen were recorded from +65° to −65° in 2.5° increments on a Philips 430 electron microscope at 200 kV. Precautions were taken to minimize specimen damage due to electron beam exposure: (i) all images were acquired digitally at a spatial resolution of 2.1 nm/pixel (with 2× binning) on a Thompson 1024 × 1024 CCD chip fiber-optically coupled to a single crystal scintillator, and (ii) the beam was blanked when images were not being acquired. Comparison of images at 0° tilt before and after acquisition of the series revealed no discernible morphological variation and about 2.06% lateral shrinkage. Images comprising the series were aligned with respect to the gold beads (1.0 nm mean alignment error) and reconstructed into the corresponding volume element according to the filtered (*r*-weighted) back-projection method.[9,25,26] Small-angle neutron scattering (SANS) was performed on unstained bulk films at Risø National Laboratory. Neutron scattering contrast was due to styrene deuteration in the copolymers.

Figure 1 is a series of transmission electron micrographs of the blends composed of copolymers with 20 (Figure 1a), 30 (Figure 1b), and 40 wt % (Figure 1c) midblock. In each of these micrographs, the minor component (isoprene) appears dark due to selective staining. The micellar (L_1) phase evident in Figure 1a is representative of the blends containing the SI0 and SI10 copolymers (not shown) and is a common characteristic of dilute block copolymer/homopolymer blends,[27] although indeterminant membrane structures have recently been reported[28] for model graft copolymer/homopolymer blends. With an increase of the midblock fraction in the copolymers employed here, the incompatible styrene and isoprene endblocks become further separated, and the driving force favoring self-organization of the block copolymers is correspondingly reduced. Moreover, since the isoprene endblocks of the copolymer molecules in these blends are effectively shielded by interfacial regions swollen with the random styrene/isoprene midblock, the blend morphology transforms from micelles to primarily unilamellar vesicles (Figure 1b), signifying the onset of the isotropic, asymmetric L_3 phase.

If this and all subsequent morphologies are presumed to be near-equilibrium (which is consistent with processing and reproducibility considerations), coexistence of micelles and vesicles in Figure 1b reveals that the transition between the L_1 and asymmetric L_3 (vesicular) phases is of first-order. As the midblock fraction is increased further (Figure 1c), the L_1 and asymmetric L_3 phases are completely replaced by a highly swollen lamellar (L_α) phase and the symmetric L_3 phase, which appears as a tightly packed and nonperiodic membrane due to its random spatial arrangement. Coexistence of the L_α and L_3 phases in Figure 1c supports existing experimental evidence[10,11,13] and theoretical predictions[12,14,15,19] that the $L_\alpha \rightarrow$ symmetric L_3 transition is likewise of first-order. While no data are available here regarding the asymmetric → symmetric L_3 transition, the morphologies seen in Figure 1 suggest that only the blends composed of extended copolymers with relatively large midblocks (≥30 wt %) exhibit regimes of morphology coexistence.

A volume reconstruction of the symmetric L_3 phase (Figure 1c), obtained from transmission electron micro-

(24) Jahn, W.; Strey, R. *J. Phys. Chem.* **1988**, *92*, 2294.

(25) Frank, J., Ed. *Electron Tomography: Three-Dimensional Imaging with the Transmission Electron Microscope*; Plenum: New York, 1992.

(26) Fung, J. C.; Liu, W.; deRuijter, W. J.; Chen, H.; Abbey, C. K.; Sedat, J. W.; Agard, D. A. *J. Struct. Biol.* **1996**, *116*, 181.

(27) Kinning, D. J.; Thomas, E. L. *J. Chem. Phys.* **1989**, *90*, 5806.

(28) Pochan, D. J.; Gido, S. P.; Pispas, S.; Mays, J. W. *Macromolecules* **1996**, *29*, 5099.

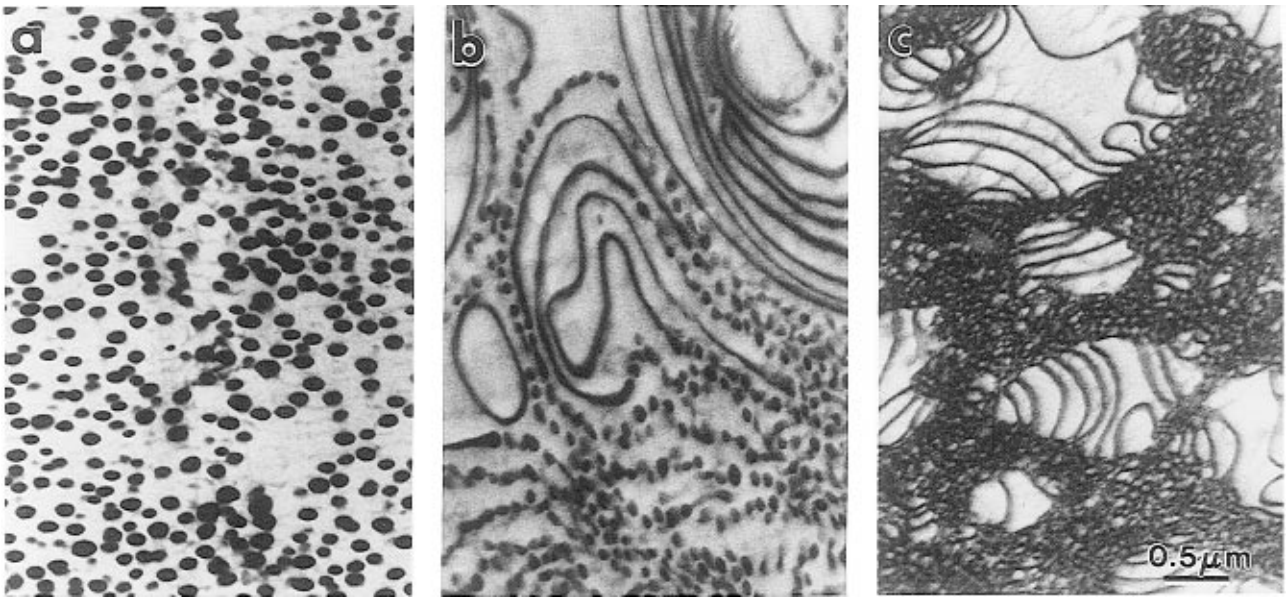

Figure 1. Transmission electron micrographs of (a) the L_1 (micellar) phase, (b) the asymmetric L_3 (vesicular) phase, and (c) coexisting L_α (swollen lamellar) and symmetric L_3 (sponge) phases in blends with copolymers possessing 20, 30 and 40 wt % styrene/isoprene midblock, respectively. Note that the morphology depends strongly on copolymer architecture in these blends of equal composition.

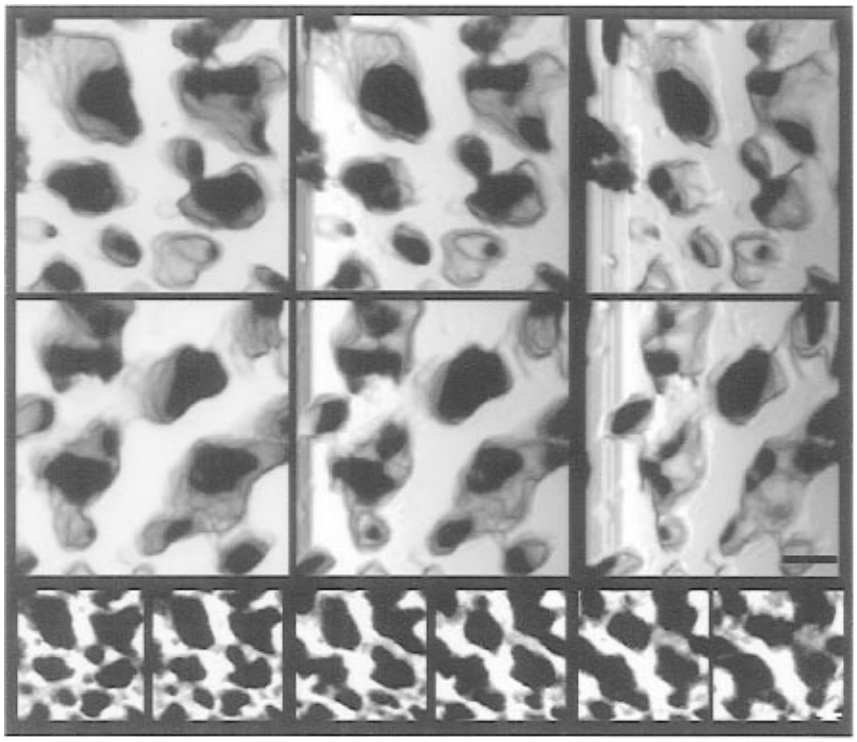

Figure 2. At the top are solid renditions of the reconstructed symmetric L_3 phase in the SI40/hPS blend. Adjacent images are displayed in 20° increments for stereoscopic viewing. Note the saddle shape and continuity of the membrane. Also shown at the bottom of this figure are sequential, contrast-reversed $x-y$ slices, each measuring *ca.* 6 nm along z (z is parallel to the electron beam), through the reconstructed L_3 phase. The polystyrene pores are as large as *ca.* 100 nm across. Scale markers in these two series are shown in the lower right image and correspond to 50 nm.

tomography,[9,25,26] is presented in Figure 2. This technique, originally developed to examine biological structures (e.g., centrosomes[29]), constitutes a powerful means by which to acquire 3-D spatial information at nanometer resolution from complex microstructural elements in-situ. At the top of Figure 2 are two series of solid renderings (in 20° angular increments, obverse and reverse) of a portion of the L_3 phase, revealing that this microstructure is a randomly connected, continuous, bilayered membrane separating comparable volumes of polystyrene homopolymer. This membrane measures 29 ± 5 nm across and is comparable in thickness to the thin isoprene-rich lamellae (36 ± 4 nm) in the swollen L_α phase (Figure 1c). Below the solid renderings in Figure 2 is a series of sequential two-dimensional slices from the solid reconstruction, illustrating that the homopolymer "pores" extend through the membrane without any discernible periodicity (in contrast to bicontinuous cubic morphologies[5−9]).

(29) Moritz, M.; Braunfeld, M. B.; Fung, J. C.; Sedat, J. W.; Alberts, B. M.; Agard, D. A. *J. Cell Biol.* **1995**, *130*, 1149.

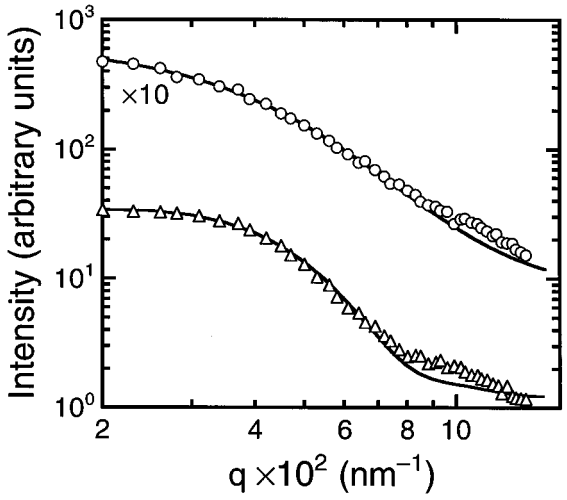

Figure 3. Small-angle neutron scattering (SANS) profiles obtained from two of the blends seen in Figure 1 (in wt % styrene/isoprene midblock): 20 (○) and 40 (△). To facilitate differentiation, the data from the SI40/hPS blend have been shifted by a factor of 10. The solid lines represent regressed fits of scattering models to the data (see the text).

The images presented in Figure 2 provide direct 3-D visualization of the symmetric L_3 morphology, as previously inferred from either scattering measurements[10,11,23] or fracture replicas of surfactant systems.[3,13] For comparison, small-angle neutron scattering profiles, displayed as intensity (I) *versus* scattering vector (q), have been measured from the blends shown in Figure 1. Even though the three $I(q)$ scattering curves clearly differ, they do not render the same unambiguous morphological conclusions as those obtained from electron microscopy. Provided in Figure 3, for instance, are the scattering data from the SI20/hPS and SI40/hPS blends. The $I(q)$ scattering function from the SI30/hPS blend is not included here since, at short length scales ($q > 0.05$ nm^{-1}), it is virtually identical to that of the SI20/hPS blend. At longer length scales (smaller q), it more closely resembles the $I(q)$ profile measured from the SI40/hPS blend.

As mentioned above, it is not possible from the scattering data alone to conclusively establish the predominant morphologies of the SI20/hPS and SI40/hPS blends. Because of the limited lower range of q (due to instrument resolution), a variety of morphology-dependent scattering models could be used to describe the rather featureless scattering curves in Figure 3. (Note that the curvature in $I(q)$ from 0.02 to 0.08 nm^{-1} in the SI20/hPS blend most likely reflects the Bessel function, which is indicative of a spherical microdomain morphology.) With the morphologies of the SI20/hPS and SI40/hPS blends known from the electron micrographs presented in Figure 1, however, appropriate scattering models may be applied to the SANS profiles in Figure 3 in order to extract quantitative microstructural dimensions.

The solid lines in Figure 3 represent least-squares fits of such models to the data (inclusive of instrumental resolution). In accord with Figure 1a, a compact-sphere model of noninteracting spherical micelles accurately represents the scattering data from the SI20/hPS blend and yields a micellar radius of about 50 nm. In the case of the nonmicellar SI40/hPS blend, models capable of describing bicontinuous microemulsions can be fitted to the scattering data in Figure 3. Fitting the model proposed by Teubner and Strey,[30] for example, to the SI40/hPS blend data yields a correlation length (ξ) on the order of 30 nm. A characteristic domain size (d) cannot, however, be discerned with any confidence from the relatively structureless experimental data.

By tailoring a series of block copolymers through systematic variation of a chemically incorporated random midblock, we have been able to adjust the phase behavior of dilute block copolymer blends at constant blend composition, copolymer chain length, and temperature. Upon an initial increase in midblock fraction, the L_1 micellar phase commonly observed[27] in dilute block copolymer/homopolymer blends gives rise to the asymmetric L_3 phase, signified by the presence of unilamellar vesicles and copolymer bilayers. As the incompatibility of the copolymer is decreased and interfacial swelling is further increased, the asymmetric L_3 transforms into the symmetric L_3 sponge phase, which consists of a randomly connected membrane. The formation of bilayered morphologies in some of the blends examined here can consequently be attributed to relatively large random copolymer midblocks.

With reduction of the copolymer/homopolymer incompatibility, the midblocks swell and rigidify the interface, thereby reducing interfacial curvature. In surfactant systems exhibiting the sponge phase, interfacial rigidity is likewise enhanced through the addition of a short-chain cosurfactant.[13] Studies of trimeric ("triple-headed") surfactants[31] in aqueous systems and graft copolymers[28] in copolymer/homopolymer blends confirm that modification of interfacial curvature yields nonclassical microstructures such as threadlike micelles and perforated layers, respectively. According to the results presented in this work, linear block copolymers can be chemically tailored to control interfacial curvature in copolymer/homopolymer blends and consequently generate complex bilayered morphologies comparable to those observed in low-molar-mass surfactant systems. This possibility has significant implications for the design of novel materials to be used in applications such as ultrafiltration or micropatterning.

Acknowledgment. J.H.L. and R.J.S. acknowledge support from the National Science Foundation (CMS-941-2361), the Shell Development Co., and the Director, Office of Energy Research, Office of Basic Energy Sciences, Materials Science Division of the U.S. Department of Energy under contract DE-AC03-76SF00098. R.J.S. also thanks the National Center for Electron Microscopy (Lawrence Berkeley Laboratory) for a Visiting Scientist Award. J.C.F., J.W.S., and D.A.A. acknowledge support from the National Institutes of Health (GM25101, J.W.S.; GM31627, D.A.A.), and D.A.A. was supported by the Howard Hughes Medical Institute. The SANS experiments were supported by the Commission of the EU through the Large Installation Plan.

LA9608876

(30) Teubner, M.; Strey, R. *J. Chem. Phys.* **1987**, *87*, 3195.
(31) Danino, D.; Talmon, Y.; Levy H.; Beinert, G.; Zana, R. *Science* **1995**, *269*, 1420.